

Published in final edited form as:

J Neuroendocrinol. 2006 November ; 18(11): 835–846. doi:10.1111/j.1365-2826.2006.01481.x.

Lack of Annexin 1 Results in an Increase in Corticotroph Number in Male but not Female Mice

J. F. Morris^{*}, S. Omer^{*}, E. Davies^{*}, E. Wang^{*}, C. John[†], T. Afzal^{*}, S. Wain^{*}, J. C. Buckingham[†], R. J. Flower[‡], and H. C. Christian^{*}

^{*}Department of Physiology, Anatomy and Genetics, University of Oxford, Oxford, UK.

[†]Department of Molecular and Cellular Neuroscience, Division of Neuroscience and Mental Health, Faculty of Medicine, Imperial College of Science Technology and Medicine, Hammersmith Hospital Campus, London, UK.

[‡]Department of Biochemical Pharmacology, William Harvey Research Institute, University of London, Charterhouse Square, London, UK.

Abstract

Annexin 1 (ANXA1) is a member of the annexin family of phospholipid- and calcium-binding proteins with a well demonstrated role in early delayed (30 min to 3 h) inhibitory feedback of glucocorticoids in the pituitary. We have examined corticotrophs in wild-type and ANXA1 knockout mice to determine the effects of lack of ANXA1 in male and female animals. Anterior pituitary tissue from ANXA1 wild-type, heterozygote and null mice was fixed and examined (i) by confocal immunocytochemistry to determine the number of corticotrophs and (ii) by electron microscopy to examine the size, secretory granule population and secretory machinery of corticotrophs. No differences in these parameters were detected in female mice. In male ANXA1 null mice, there were approximately four-fold more corticotrophs than in wild-type animals. However, the corticotrophs in ANXA1 null mice were smaller and had reduced numbers of secretory granules (the reduction in granules paralleled the reduction in cell size). No differences in the numerical density of folliculo-stellate, gonadotroph, lactotroph or somatotroph cells were detected in male ANXA1 null mice. Plasma corticosterone, adrenocorticotrophic hormone (ACTH) and pituitary pro-opiomelanocortin mRNA were unchanged but pituitary ACTH content was increased in male ANXA1 null mice. Interleukin (IL)-6 pituitary content was significantly elevated in male and reduced in female ANXA1 null mice compared to wild-type. In conclusion, these data indicate that ANXA1 deficiency is associated with gender-specific changes in corticotroph number and structure, via direct actions of ANXA1 and/or indirect changes in factors such as IL-6.

Keywords

corticotrophs; annexin 1 knockout mouse; glucocorticoids

The hypothalamo-pituitary-adrenal axis (HPA) plays an essential role in the maintenance of homeostasis. In normal circumstances, its activity is tightly regulated with changes in glucocorticoid secretion occurring in accordance with the circadian rhythm and in conditions of stress. Sex differences in HPA activity are well documented and a number of studies have demonstrated that gonadal steroids act as regulators of HPA activity. Sexual dimorphism in

corticosterone secretion was first reported by Kitay (1) and, subsequently, several groups confirmed elevated corticosterone secretion in basal and some stress conditions in female rodents relative to males (2, 3). Oestrogen exerts stimulatory effects on stress-induced adrenocorticotrophic hormone (ACTH) and glucocorticoid release, whereas testosterone acts to inhibit HPA activity (3). In the rat, there is evidence that changes in plasma corticosterone are associated with oestrous cycle stage: peak ACTH and corticosterone levels are highest in the afternoon of pro-oestrous (4), the time of maximal oestradiol secretion (5). Furthermore, the stress responsiveness of the female rat HPA is known to vary with the oestrous cycle, with increased corticosterone release in response to stress at pro-oestrous (6). In addition to the established effects of sex steroids on HPA function in the rat in adulthood, it is now evident that exposure to gonadal steroids influences HPA programming during perinatal development (7) and is responsible for the pubertal shift in HPA responsiveness (8).

Annexin 1 (ANXA1) is a glucocorticoid-regulated protein that has been implicated in the regulation of phagocytosis, cell signalling and proliferation, as a mediator of glucocorticoid action in inflammation, and in the control of anterior pituitary hormone release (9, 10). ANXA1 is found in abundance in the anterior pituitary gland, particularly in the agranular S-100-positive folliculo-stellate (FS) cells (11). Functional studies have identified a key role for ANXA1 in effecting certain acute, nontranscriptional inhibitory actions of the glucocorticoids on the release of corticotrophin (ACTH) (12-14). The initial effect of glucocorticoids in several tissues, including the anterior pituitary, is to cause phosphorylation and externalisation of ANXA1 from the cytoplasm to the outer cell surface where it is retained by a Ca^{2+} -dependent mechanism (15-17). Subsequently, the steroids induce *de novo* ANXA1 synthesis to replenish the intracellular stores of the protein (16). Functional and binding studies suggest that the glucocorticoid-induced externalisation of ANXA1 via an ATP-binding cassette transporter (18) is an important mechanism that enables the protein to access binding sites (19) on the surface of the corticotrophs and thereby to exert paracrine regulation of the release of ACTH. Our finding that the FS cells are the principal source of ANXA1 in the anterior pituitary gland (11) and evidence that FS cells are rich in glucocorticoid receptors (20) are both consistent with the proposal that ANXA1 is a paracrine mediator of glucocorticoid action. FS cells form an extensive functional intrapituitary circuitry via which information can be transferred (21) and pituitary hormone secretion modulated through the release of several bioactive molecules, including cytokines and growth factors [e.g. follistatin, interleukin (IL)-6, macrophage migration inhibitory factor and leukaemia inhibitory factor] in addition to ANXA1 (22-24). Release of many of these factors is also regulated by glucocorticoids and sex steroids (24, 25).

To explore further the role of ANXA1, ANXA1 null mice have recently been generated (26). In models of experimental inflammation, ANXA1 null mice exhibit a prolonged and exacerbated inflammatory response and are partially resistant to the anti-inflammatory properties of glucocorticoids (26-28). Furthermore, gender differences were evident in that the male ANXA1 null leucocyte response to an inflammatory episode was enhanced to a greater extent than the female response (26). In the present study, we have used ANXA1 null mice to explore further the role of this mediator in HPA axis regulation by analysing the morphological secretion-related characteristics of the anterior pituitary corticotrophs.

Materials and methods

Animals

ANXA1 null mice were generated by targeting of the *ANXA1* gene in embryonic stem (ES) cells as previously described (26). Gene targeting was performed by homologous recombination in ES cells derived from strain 129 Agouti mice. Correctly targeted ES cells were then injected into blastocysts from C57 Black females. The resulting chimaeric males

were test-bred with C57 Black females to produce (129 × C57) F₁ offspring, which were then mated together to produce the F₂ homozygous knockout animals used in the present study. Male and female wild-type littermate controls, ANXA1 heterozygote and ANXA1 null mice (20–25 g body weight) were maintained on a standard chow pellet diet with tap water *ad lib*. Animals were housed in groups of six per cage in a quiet room under a 12 : 12 h light/dark cycle (lights on 08.00 h) and temperature was maintained at 21–22 °C. All experiments were started between 08.00 h and 09.00 h to avoid changes associated with the circadian rhythm. The Principles of Laboratory Animal Care (NIH Publication no. 85-23) were followed and animal work was carried out under license in accordance with the UK Guidance on the Operation of Animals, Scientific Procedures Act 1986. Anterior pituitary tissue was collected immediately after decapitation for determination of ACTH content, pro-opiomelanocortin (POMC) mRNA and electron microscopy of endocrine cells. For ACTH analysis, anterior pituitaries were homogenised using brief sonication in 250 μ l of ice-cold 5 N acetic acid with 2 mg/ml bovine serum albumin. Trunkal blood was also collected for determination of plasma ACTH and corticosterone concentrations. For electron microscopy, anterior pituitary tissue was immersion fixed in freshly prepared 3% w/v freshly prepared formaldehyde, 0.05% v/v glutaraldehyde (VWR International Ltd, Lutterworth, UK) in phosphate-buffered saline (PBS), pH 7.2 for 3 h at 4 °C.

For analysis of FS cells, mice were terminally anaesthetised by intraperitoneal injection of 3 mg sodium pentobarbital (Sagatal, Rhone Merieux, France) and perfused through the heart with heparinised saline (0.9% NaCl and 10 U/ml heparin) followed by 3% paraformaldehyde and 0.05% glutaraldehyde in PBS. In nonperfused pituitary tissue, the intimate cell-to-cell contacts make visualisation of FS cells difficult. However, in perfusion-fixed material, the cells become separated allowing the processes to be seen clearly. The pituitary gland was removed and immersed in the same fixative for 3 h at 4 °C and prepared for electron microscopy as described below.

Reverse transcriptase-polymerase chain reaction (RT-PCR) for POMC mRNA

Total RNA was isolated using RNeasy mini kit (Qiagen, Hilden, Germany) following the manufacturer's instructions, eluted in 40 μ l water and treated with DNase (DNA-free; Ambion, Witney, UK) to remove traces of genomic DNA contamination. A total of 3.5 μ g of RNA from each sample was subsequently reverse transcribed using 1 μ l MMLV reverse transcriptase (Clontech, Oxford, UK), 2 μ l 10 mM dNTP, 2 μ l 100 mM DTT in a total volume of 20 μ l. POMC primer sequences were: forward primer, 5' - AGATGGCAGTCCAGAGCCGAGTCC-3'; reverse primer, 5' - TGGCCCTTCTGTGCGGTTCTT-3' (with an expected size of 377 bp). Each reaction also contained primers for GAPDH which served as an internal control: forward primer 5' - ACTCACGGCAAATTCAACGGCACAG-3'; reverse primer 5' - TGGTCATGAGCCCTTCCACAATGCC-3' (expected size 376 bp; all primers synthesised by Sigma-Genosys, Hinxton, UK). 1 μ l cDNA was used as a template in the PCR reactions (total volume 50 μ l). PCR conditions were optimised to an annealing temperature of 63 °C and 29 cycles (Expand High Fidelity PCR system; Roche, Hemel Hempstead, UK). A negative control PCR was also run using the primers but omitting the cDNA in the reaction tube. PCR products were separated on a 1% agarose gel stained with ethidium bromide, photographed and analysed by scanning densitometry (TINA software version 2.10, Raytest Isotopenmessgeraete GmbH, Straubenhardt, Germany).

ACTH enzyme-linked immunosorbent assay (ELISA) and corticosterone radioimmunoassay

ACTH was determined in duplicate by use of a commercially available ELISA (IDS Ltd, Tyne and Wear, UK) according to the manufacturer's instructions. The assay sensitivity was

0.5 pg/ml and the inter- and intra-assay coefficients of variation were 3.1% and 5.8%, respectively. The assay is specific for full-length ACTH₁₋₃₉ and does not detect ACTH cleavage products. Plasma corticosterone was determined in duplicate by use of a commercially available radioimmunoassay (IDS Ltd), according to the manufacturer's instructions. The intra- and inter assay variation of the assay were 10.4% and 12.4%, respectively.

Electron microscopy

Anterior pituitary tissue was prepared for electron microscopy by standard methods. Briefly, segments of fixed anterior pituitary were stained with uranyl acetate (2% w/v in distilled water), dehydrated through increasing concentrations of methanol (70–100%) at –20 °C and embedded in LR Gold acrylic resin (London Resin Company Ltd, Reading, UK). Ultrathin sections were prepared and mounted onto formvar-coated mesh nickel grids (Agar Scientific Ltd, Stanstead, UK).

Endocrine cells in sections taken systematically from different depths of the embedded tissue were identified on the basis of their secretory granule populations (shape, electron density, size and distribution), and organelle structure, nucleus size and chromatin characteristics. Immunogold labelling for ACTH, prolactin (PRL), luteinising hormone (LH), growth hormone (GH) and S-100 was also performed to assist with the identification of corticotrophs, lactotrophs, gonadotrophs, somatotrophs and FS cells, respectively (29). Both type I and type II lactotrophs were analysed: type I lactotrophs contain small numbers of large (> 250 nm diameter) irregularly shaped granules; type II lactotrophs contain large numbers of small (< 150 nm diameter) spherical granules (30). Sections were incubated with either rabbit anti-rat ACTH polyclonal antibody (1 : 250), rabbit anti-rat PRL (1 : 5000), guinea-pig anti-rat LH (1 : 3000), monkey anti-rabbit GH (1 : 5000; all from the National Hormone and Pituitary Programme, Torrance, CA, USA) or sheep anti-S-100 (1 : 400; Dako Corp, Cambridge, UK) for 2 h and for 1 h with either anti-rabbit immunoglobulin (Ig)G 15 nm gold complex (ACTH, PRL) or Protein A-15 nm gold complex (LH, GH, S-100; gold conjugates from British Biocell, Cardiff, UK). For control sections, the primary antibody was omitted and replaced with 0.1 M phosphate buffer containing 1% w/v egg albumin. Sections were then lightly counterstained with uranyl acetate and lead citrate. All antibodies were diluted in 0.1 M phosphate buffer containing 1% w/v egg albumin. The sections were viewed with a JEOL 1010 transmission electron microscope (JEOL, Peabody, MA, USA). The proportion of each cell type in wild-type and ANXA1 null pituitary was determined. For each pituitary (n = 4), four randomly orientated sections each containing ten grid squares of intact tissue were assessed. The density of each cell population was determined by counting the number of each cell type divided by the total number of cells per grid.

Electron microscopy morphological studies

For analysis of cell morphology by point counting (31), ten micrographs of each cell type (corticotrophs, type I and II lactotrophs, somatotrophs, gonadotrophs and FS cells) per animal were taken at a magnification of × 4000. The negatives were scanned into Adobe Photoshop, version 5.5 (Adobe Systems Incorporated, San Jose, CA, USA) and printed onto A4 paper for analysis at × 2.77 linear magnification (final linear magnification 1 μm = 1.11 cm). In all cases, the analyst was blind to the sample code. The following parameters were calculated from endocrine cell micrographs: cytoplasmic, nuclear and total cell areas; granule diameter and density; relative density of rough endoplasmic reticulum and dilation of Golgi apparatus. Sections from four animals per group were examined. To determine total and nuclear cell areas a 1-cm grid acetate sheet was placed at random over the cell and the number of grid intersections that overlaid the cell was recorded. Cytoplasmic area was determined by subtracting nuclear area from total cell area. The data obtained was

multiplied by an areal conversion factor of 1.23 because, on each micrograph, 1 cm² represented 1.23 μm². Mean granule diameter was determined by the overlay and match of circles of known diameter onto granules in the cell for 30 granules per cell. To determine granule areal density, a 0.7-cm grid was used: the number of intersections that overlaid a granule was counted, adjusted by the areal conversion factor and divided by the cytoplasmic area of the cell. Expansion of the rough endoplasmic reticulum (rER) and Golgi apparatus was assessed visually and graded on a scale of 0–4 (0, no expansion; 4, the most expansion). These estimates do not provide absolute measurements but do provide a basis for comparison. The total, cytoplasmic and nuclear areas of FS cells were analysed from scanned micrographs using Image J software (US National Institutes of Health, Bethesda, MD, USA; <http://rsb.info.nih.gov/ij>).

Fluorescence microscopy

For visualisation of corticotrophs by immunofluorescence semithin (100 μm) sections of LR Gold-embedded anterior pituitary tissue were prepared onto glass slides. Sections were rinsed in PBS, blocked with 10% foetal calf serum (FCS) in PBS at room temperature for 1 h and incubated for 2 h with rabbit anti-rat ACTH polyclonal antibody (National Hormone and Pituitary Programme, Torrance, CA, USA) at a dilution of 1 : 250 in 10% FCS in PBS. Immunoreacted sections were washed with PBS then incubated for 1 h at room temperature with a fluorescein-conjugated goat antirabbit IgG (Vector Laboratories Inc, Burlingame, CA, USA). The slides were mounted in Vectashield mounting medium containing propidium iodide (Vector Laboratories Inc, Burlingame, CA, USA) to counterstain cell nuclei. Sections were then examined using a TCS confocal microscope (Leica Corp. Microsystems, Wetzlar GmbH, Germany). The numerical density of corticotrophs in the pituitary was quantified by counting the number of ACTH immuno-positive cells per 250 μm × 250 μm of section determined using Axiovision 4.2 Image analysis software (Zeiss, Welwyn Garden City, UK). Four sections taken from different depths of the tissue block were quantified per animal.

Detection of IL-6 by Western blot analysis

IL-6 was extracted from pituitary tissue by sonication (25 Hz, 20 s, Soniprep 150, MSE, UK) on ice in EDTA (10 mM) containing Triton X-100 (1% v/v, Sigma Chemical Co.) and the total protein content of each sample determined by the Bradford assay. The extracted proteins were separated by 10% SDS-PAGE [20 μg/channel in a volume of 20 μl by use of a midgel gel Hoeffer electrophoresis system and power pack (LKB, Milton Keynes, UK)] and transferred electrophoretically to nitrocellulose paper (Bio-Rad laboratories Inc. Ltd, Hemel Hempstead, UK). IL-6 was detected by overnight incubation (4 C) with a rabbit anti-IL-6 polyclonal antibody (diluted 1 : 1000; Abcam, Cambridge, UK) followed by antirabbit IgG conjugated to horseradish peroxidase (diluted 1 : 5000; Sigma Chemical Co., Poole, UK) and visualised by ECL (Amersham Biosciences, Little Chalfont, Bucks, UK). The blots were scanned using a flatbed scanner (HP Scanjet 5200 with Adobe Photodeluxe Business Edition v1.1) and the band intensity analysed using the TINA software programme (TINA version 2.10, Raytest Isotopenmessgeraete GmbH, Germany). Leukaemia inhibitory factor (LIF) was also detected in samples using the same method with rabbit anti-LIF primary antibody (R and D Systems, Abingdon, UK) and antirabbit IgG peroxidase conjugated secondary antibody, and the housekeeping protein β-actin with a monoclonal anti-β-actin clone AC-15 (1 : 5000) and peroxidase-conjugated antimouse secondary antibody (1 : 5000; all Sigma Chemical Co., Poole, UK).

Immunogold detection of IL-6

Male and female wild-type and ANXA1 null pituitary tissues, fixed in a mixture of freshly prepared 3% formaldehyde and 0.05% glutaraldehyde in PBS for 4 h at 4 C, were washed

briefly in PBS, and transferred to a solution of 2.3 M sucrose in PBS overnight. The cryoprotected tissue was cut into 300- μm -thick slices with a Vibroslice (Camden Instruments, Sileby, UK), slam-frozen (Reichert MM80E; Leica, Milton Keynes, UK), freeze-substituted at -80 C in methanol for 48 h, and embedded at -20 C in LR Gold acrylic resin (London Resin Company Ltd, Reading, UK) in a Reichert freeze-substitution system. Ultrathin sections were prepared by use of a Reichert Ultracut S ultratome, mounted onto formvar-coated nickel grids, incubated for 2 h with anti-IL-6 polyclonal antibody (dilution, 1 : 400; Abcam, Cambridge, UK) and for 1 h with antirabbit IgG-15 nm gold complex, followed by 2 h with anti-S-100 (a FS cell marker) polyclonal antibody (dilution, 1 : 4000; DAKO Corp., Cambridge, UK) and for 1 h with antisheep IgG-5 nm gold complex, then lightly counterstained with uranyl acetate and lead citrate. All antibodies were diluted in 0.1 M phosphate buffer containing 0.1% w/v egg albumin. For control sections, the primary antibodies were omitted and replaced with 0.1 M phosphate buffer containing 0.1% w/v egg albumin. Sections were examined with a JEOL 1010 transmission electron microscope. The number of 15 nm gold particles was counted in ten cells/-animal and calculated as particles/ μm^2 by dividing the total number of gold particles counted by the cytoplasmic area.

Statistical analysis

All morphometric values represent the mean \pm SEM ($n = 4$ animals per group). Preliminary analysis confirmed that the data were normally distributed. Subsequent analysis was undertaken by one-way ANOVA with *post hoc* analysis performed using the Bonferroni test. Semi-quantitative measures of IL-6 were made by comparisons of Western blot band optical densities (arbitrary units). ANXA1 null expression was expressed as a percentage of the wild-type of the same gender and expressed as the mean \pm SEM ($n = 4$ gels); statistical comparisons between the normally distributed groups were made by Student's t-test. For ACTH and corticosterone hormone data, preliminary analysis by the Shapiro and Wilks test confirmed that the data were normally distributed. Subsequent analysis was performed by two-way ANOVA with *post hoc* comparisons by Scheffe's test. Data was expressed as mean \pm SEM ($n = 8$ animals). In all cases, $P < 0.05$ was considered statistically significant.

Results

Basal hypothalamo-pituitary-adrenal axis activity

Figure 1 demonstrates the amount of anterior pituitary POMC mRNA, ACTH content, circulating ACTH and corticosterone measured in wild-type and ANXA1 null mice. POMC and GAPDH mRNA was detected as appropriately sized bands by RT-PCR whereas the negative control reactions yielded no band (Fig. 1a,b). No difference in the amount of anterior pituitary POMC mRNA in wild-type and ANXA1 null mice was detected. However, anterior pituitary ACTH content was significantly greater ($P < 0.05$) in ANXA1 null male mice compared to wild-type but no significant difference was measured between female ANXA1 null male mice and wild-type (Fig. 1c). No significant differences were measured in circulating basal ACTH (Fig. 1d) or corticosterone (Fig. 1e) in wild-type and ANXA1-null mice.

Corticotroph morphology

Electron microscopic analysis of corticotroph morphometric parameters are shown in Figs 2 and 3. In all of the morphometric parameters measured, there was no difference measured between female wild-type, heterozygote and ANXA1 null mice (Figs 2a-c and 3a-e). By contrast, total cell area (Fig. 2a), cytoplasmic area (Fig. 2b) and nuclear area (Fig. 2c) were all significantly ($P < 0.01$) reduced in ANXA1 null male mice compared to wild-type. Nuclear area was also significantly ($P < 0.05$) reduced in heterozygote male corticotrophs compared to wild-type (Fig. 1c) but male heterozygote cell area (Fig. 2a) and cytoplasmic

area (Fig. 2b), although reduced in mean size, were not significantly different to wild-type corticotrophs. Granule area was significantly ($P < 0.05$) reduced in ANXA1 null male mice compared to wild-type (Fig. 3a) but, when the reduction in ANXA1 null cytoplasmic area was taken into account, no significant difference was detected in the numerical density of corticotroph granules between wild-type and ANXA1 null mice (Fig. 3b). Granule diameter was not affected in heterozygote or ANXA1 null corticotrophs (Fig. 3c). rER (Fig. 3d) and Golgi apparatus (Fig. 3e) were both significantly reduced in ANXA1 null compared to wild-type male corticotrophs. Figure 4 shows electron micrographs of anterior pituitary from wild-type and ANXA1 null mice. In wild-type mice, corticotrophs were stellate, single and characterised by pale cytoplasm and peripheral secretory granules (Fig. 4a). In male ANXA1 null mice, many more immunoidentified corticotrophs were present, often in clusters (Fig. 4b). Analysis of corticotroph cell density by immunofluorescence microscopy confirmed these observations (Fig. 5). Figure 5(a) illustrates the distribution of single corticotrophs in a section of wild-type male anterior pituitary, whereas many clusters of corticotrophs are visible in ANXA1 null male anterior pituitary (Fig. 5b). Quantification of corticotroph cell density in this tissue (Fig. 5c) revealed a significant ($P < 0.01$) 4.4-fold increase in the corticotrophs of male ANXA1 null mice compared to wild-type mice with data for heterozygotes intermediate between wild-type and null mice. By contrast, no significant difference in corticotroph cell density was detected among female wild-type, heterozygote and ANXA1 null mice (Fig. 5c).

Folliculo-stellate cell morphology

Electron microscopic analysis of FS cell morphometric parameters is shown in Fig. 6. Electron micrographs demonstrate, after perfusion fixation, the characteristic ultrastructural appearance of FS cells with elongated cytoplasmic processes but no secretory granules in wild-type male (Fig. 6a) and ANXA1 null (Fig. 6b) male mice. Cell (Fig. 6c) and cytoplasmic (Fig. 6e) area were significantly greater in male and female ANXA1 null FS cells compared to wild-type ($P < 0.01$) whereas nuclear area (Fig. 6d) was significantly greater in male but not female ANXA1 null FS cells ($P < 0.01$). Quantification of FS cell density (Fig. 6f) revealed no significant difference in the FS cell density in male or female wild-type and ANXA1 null anterior pituitary.

Lactotroph, gonadotroph and somatotroph morphology

Electron microscopic analysis of lactotrophs, gonadotroph and somatotroph cell morphometric parameters in male wild-type and ANXA1 null mice is shown in Table 1. In all of the morphometric parameters, excepting rER, there was no difference measured between wild-type and ANXA1 null mice. rER was significantly increased in ANXA1 null compared to wild-type lactotrophs, gonadotrophs and somatotrophs. Analysis of cell density of lactotrophs, gonadotrophs and somatotrophs revealed no significant differences between wild-type and ANXA1 null anterior pituitary (Table 1). No significant difference was measured in total cell number per grid square between wild-type and ANXA1 null anterior pituitary (data not shown).

IL-6 expression in the pituitary gland

IL-6 was readily detected as a single 24-kDa immunoreactive band by Western blotting. Figure 7 demonstrates that IL-6 expression was significantly increased ($P < 0.01$) in male ANXA1 null mice compared to wild-type (Fig. 7a, lanes 3 and 4 versus lanes 1 and 2; Fig. 7E) but, in contrast, was significantly decreased ($P < 0.05$) in female ANXA1 null mice compared to wild-type (Fig. 7b, lanes 3 and 4 versus lanes 1 and 2; Fig. 7f). No change was observed in the amount of β -actin detected in male (Fig. 7c) or female (Fig. 7d) extracts (lanes 1 and 2 wild-type versus lanes 3 and 4 ANXA1 null). IL-6 was also readily detected in freeze-substituted anterior pituitary tissue from wild-type (Fig. 8a) and ANXA1 null mice

(Fig. 8b) by immunogold labelling. The IL-6 immunoreactivity was localised exclusively to the cytoplasm of the FS cells, which were identified by morphological criteria and S-100 labelling (Fig. 8). Quantitative analysis of the IL-6 labelling by counting the gold particles confirmed the semiquantitative densitometry data obtained from Western blot analysis (Table 2). No significant difference in the anterior pituitary expression of LIF was detected when comparing wild-type and ANXA1 null tissues by Western blot analysis, immunogold labelling and electron microscopy (data not shown).

Discussion

In the present study, we demonstrate that a lack of ANXA1 is associated with a dramatic increase in corticotroph density, but not FS cell, gonadotroph, lactotroph or somatotroph density, in the anterior pituitary of male mice. The expansion of the corticotroph population was accompanied by a general decrease in corticotroph cell dimensions (i.e. cell, nuclear, cytoplasmic area) and a reduced total area of granules. The reduced granule content of individual corticotrophs is likely to indicate decreased production of ACTH in view of the decrease in both cell size and rough endoplasmic reticulum. The male heterozygotes had intermediate values of corticotroph dimensions, suggesting a dose-dependent effect of the ANXA1 gene. By contrast, somatotroph, gonadotroph and lactotroph morphology was not obviously affected by ANXA1 knockout excepting a relatively subtle change of an increase in the amount of rER. The effects on corticotrophs of ANXA1 knockout were gender specific because no significant changes in female corticotroph parameters could be detected.

The clustering of corticotrophs in the male ANXA1 null pituitary strongly suggests that cell proliferation was the cause of the approximately four-fold increase in corticotrophs. Corticotroph turnover is dependent on the mitogenic actions of corticotropin-releasing hormone (CRH) (32-34) and the antiproliferative and proapoptotic actions of glucocorticoids (35). The striking increase in corticotrophs in male ANXA1 null mice initially suggested that in males, but not females, a lack of ANXA1-mediated glucocorticoid feedback at the hypothalamus (36) had increased CRH secretion causing proliferation of corticotrophs. However, paraventricular nucleus CRH expression was not altered in male or female wild-type or ANXA1 null mice (J. C. Buckingham and C. John, personal communication), although it is possible that corticotroph sensitivity to CRH could have increased.

The increase in corticotroph proliferation could arise directly as a result of ANXA1 deficiency because ANXA1 exerts both the antiproliferative (37, 38) and pro-apoptotic (39) actions of glucocorticoids. There is strong evidence for ANXA1 inhibition of cell proliferation (40-43) and ANXA1-binding sites have been identified on the surface of corticotrophs (19), which may be related to the FPR receptor family implicated in ANXA1 signalling (44, 45). Therefore, increased proliferation in the ANXA1 null mice could have been mediated via the lack of ANXA1 actions to directly inhibit signalling, or indirectly inhibit secretion, of a juxtacrine or paracrine proliferation or pro-apoptotic signal from another anterior pituitary cell type. Factors within the anterior pituitary gland that play an important role in the regulation of corticotroph proliferation, include epidermal growth factor (46), leukemia inhibitory factor (LIF) and IL-6 (47, 48) derived from FS cells, macrophages and T cells. We therefore measured pituitary content of LIF and IL-6 in wild-type and ANXA1 null mice by Western blot analysis and immunogold electron microscopy. Although no differences were measured in LIF content, pituitary IL-6 content was elevated in male ANXA1 null mice and reduced in female ANXA1 null mice compared to wild-type. Immunogold electron microscopy confirmed these findings and localised IL-6 exclusively to the cytoplasm of FS cells. It therefore is possible that the increased corticotroph population in male ANXA1 null mice is secondary to chronic changes in FS cell IL-6 production.

However, although pituitary IL-6 content was decreased in female ANXA1 null mice, no change in corticotroph number was measured compared to wild-type. Because FS cells are the principal source of ANXA1 in the anterior pituitary gland, changes in the number and/or morphology of FS cells might also have been expected. Although FS number was not affected, FS cell size was increased in male and female ANXA1 null tissue suggesting increased cell activity.

From the present study, it is not clear when the increase in number of corticotrophs occurred. The corticotrophs are the first hormone-producing cells of the pituitary to reach terminal differentiation. Expression of POMC starts in corticotrophs at about day 12.5 of embryonic development in the mouse (49) following the expression of the transcription factors Tpit-1/Tbx19 and NeuroD1 (50). It is possible that changes occurred at this point to regulate the differentiation and/or proliferation of progenitor cells. It is also possible that the expansion of the corticotroph population in the ANXA1 null mice occurred postnatally because the adult corticotroph population is surprisingly labile; for example, acute stress by a novel environment has been shown to increase the rat corticotroph population by 20% (51).

Despite the abundant evidence that ANXA1 plays a role in glucocorticoid feedback in the pituitary, gene deletion does not appear to affect feedback. Although thymic weights are reduced in tissue mass in relation to body weight in ANXA1 null mice (52), breeding statistics and growth are normal (26) and there are no obvious signs of hypercortism. Circulating basal ACTH secretion, corticosterone secretion and the amount of anterior pituitary POMC mRNA were unchanged in ANXA1 null male mice despite the expansion of the corticotroph population in these animals. However, pituitary ACTH content was elevated in male ANXA1 pituitary although the other HPA axis parameters had maintained homeostasis. There was no alteration in the basal HPA axis function in female ANXA1 null mice and no significant change in the ACTH content, number or morphology of the corticotrophs. It is a little more difficult to link the reduction in the size and secretory granule population in ANXA1 null male mice with the functional data and IL-6 pituitary content data. It would appear likely that the increase in basal IL-6 in male ANXA1 null mice represents more production and secretion of IL-6 that would act directly to stimulate ACTH release (53, 54) and therefore would be expected to increase the activity of the corticotrophs. However, the reduction in granule profile area indicates a reduction in the total number of granules per corticotroph because the average individual granule diameter and granule areal density remain unchanged and rER and Golgi apparatus had declined. Therefore, it is most likely that the ACTH content of the corticotroph population as a whole is increased because of the increased numbers of corticotrophs. One reason for the lack of effect of ANXA1 deletion on feedback control of ACTH may be functional redundancies amongst members of the annexin protein family. In the anterior pituitary, the absence of ANXA1 has been shown to be accompanied by an increase in expression of Annexin IV but its function is as yet unexplored (52).

Sex hormones or gender differences are well known to influence the inflammatory response, basal cytokine release and the responsiveness of the HPA axis to stress (1-8, 26). The mechanisms that underly the absence of an effect of ANXA1 deletion on the corticotroph population in females are unknown. However, it is likely that gonadal factors contribute to the gender difference observed in pituitary IL-6 content and corticotroph population size in ANXA1 null mice, and to the sexual dimorphism previously reported in the ANXA1 null mouse leucocyte response to inflammation (26). The gonadal status of the male and female animals and their genital tracts were not grossly different in the ANXA1 null mice (52). It is possible that, in males, testosterone influences corticotroph number directly in the absence of putative inhibition by ANXA1 although, to our knowledge, corticotroph expression of

androgen receptors has not been investigated. We are currently exploring the hypothesis that gonadal factors contribute to the sexual dimorphism in ANXA1 biology by examining the effects of gonadectomy and steroid replacement on the mouse phenotype.

In conclusion, these data indicate that ANXA1 deficiency is associated with gender-specific changes in corticotroph number and structure, via direct actions of ANXA1 and/or indirect changes in factors such as IL-6. ANXA1 therefore appears to coordinate the balance of cell growth and number in the anterior pituitary. Although homeostasis of basal HPA function was achieved in the ANXA1 null mouse, it is possible that ANXA1 may contribute physiologically to the dimorphic HPA response between the sexes. The experiments described here will prompt further investigations into the mechanism of ANXA1 regulation of corticotroph cell number.

Acknowledgments

We thank Lynne Scott and Sarah Rodgers for expert technical support. Research in the authors' laboratory is supported by the Wellcome Trust.

References

1. Kitay JI. Sex differences in adrenal cortical secretion in the rat. *Endocrinology*. 1961; 68:818–824. [PubMed: 13756461]
2. Critchlow V, Liebelt RA, Bar-Sela M, Mountcastle W, Lipscomb HS. Sex difference in resting pituitary-adrenal function in the rat. *Am J Physiol*. 1963; 205:807–815. [PubMed: 4291060]
3. Seale JV, Wood SA, Atkinson HC, Bate E, Lightman SL, Ingram CD, Jessop DS, Harbuz MS. Gonadectomy reverses the sexually diergic patterns of circadian and stress-induced hypothalamo-pituitary-adrenal axis activity in male and female rats. *J Neuroendocrinol*. 2004; 16:516–524. [PubMed: 15189326]
4. Carey MP, Deterd CH, de Koning J, Helmerhorst F, deKloet ER. The influence of ovarian steroids on hypothalamic-pituitary-adrenal regulation in the female rat. *J Endocrinol*. 1995; 144:311–321. [PubMed: 7706984]
5. Freeman, ME. The ovarian cycle of the rat. In: Knobil, E.; Neill, JD., editors. *The Physiology of Reproduction*. Vol. 2. New York, NY: Raven Press; 1988. p. 1893-1928.
6. Viau V, Meaney MJ. Variations in the hypothalamic-pituitary-adrenal response to stress during the estrous cycle in the rat. *Endocrinology*. 1991; 129:2503–2511. [PubMed: 1657578]
7. Seale JV, Wood SA, Atkinson HC, Lightman SL, Harbuz MS. Organizational role for testosterone and estrogen on adult hypothalamic-pituitary-adrenal axis activity in the male rat. *Endocrinology*. 2005; 146:1973–1982. [PubMed: 15625243]
8. Viau V, Bingham B, Davis J, Lee P, Wong M. Gender and puberty interact on the stress-induced activation of parvocellular neurosecretory neurons and corticotrophin-releasing hormone messenger ribonucleic acid expression in the rat. *Endocrinology*. 2005; 146:137–146. [PubMed: 15375029]
9. Ahluwalia, A.; Buckingham, JC.; Croxtall, JD.; Flower, RJ.; Goulding, NJ.; Perretti, M. Biology of annexin I. In: Seaton, BA., editor. *Annexins: Molecular Structure to Cellular Function*. Austin, TX: RG Landes; 1996. p. 161-199.
10. John CD, Christian HC, Morris JF, Flower RJ, Solito E, Buckingham JC. Annexin I and the regulation of endocrine function. *Trends Endocrinol Metab*. 2004; 15:103–109. [PubMed: 15046738]
11. Traverso V, Christian HC, Morris JF, Buckingham JC. Lipocortin 1 (Annexin I): a candidate paracrine agent localized in pituitary folliculo-stellate cells. *Endocrinology*. 1999; 140:4311–4319. [PubMed: 10465305]
12. Taylor AD, Cowell A-M, Flower RJ, Buckingham JC. Lipocortin 1 mediates an early inhibitory action of glucocorticoids on the secretion of ACTH by the rat anterior pituitary gland *in vitro*. *Neuroendocrinology*. 1993; 58:430–439. [PubMed: 7506818]

13. Taylor AD, Loxley HD, Flower RJ, Buckingham JC. Immunoneutralization of lipocortin 1 reverses the acute inhibitory effects of dexamethasone on the hypothalamo-pituitary-adrenocortical responses to cytokines in the rat *in vitro* and *in vivo*. *Neuroendocrinology*. 1995; 62:19–31. [PubMed: 7566434]
14. Taylor AD, Christian HC, Morris JF, Flower RJ, Buckingham JC. An antisense oligodeoxynucleotide to lipocortin 1 reverses the inhibitory actions of dexamethasone on the release of ACTH from rat pituitary tissue *in vitro*. *Endocrinology*. 1997; 138:2909–2918. [PubMed: 9202235]
15. Chapman LP, Nishimura A, Buckingham JC, Flower RJ, Morris JF, Christian HC. Externalisation of annexin I from a folliculo-stellate, TtT/GF, cell line. *Endocrinology*. 2002; 143:4330–4338. [PubMed: 12399429]
16. Philip JG, Flower RJ, Buckingham JC. Glucocorticoids modulate the cellular disposition of lipocortin 1 in the rat brain *in vivo* and *in vitro*. *Neuroreport*. 1997; 8:1871–1876. [PubMed: 9223068]
17. Solito E, Mulla A, Morris JF, Christian HC, Flower RJ, Buckingham JC. Dexamethasone induces rapid serine phosphorylation and membrane translocation of annexin 1 in a human folliculostellate cell line via a novel nongenomic mechanism involving the glucocorticoid receptor, protein kinase C, phosphatidyl 3-kinase and mitogen activated protein kinase. *Endocrinology*. 2003; 144:1164–1174. [PubMed: 12639897]
18. Chapman LP, Epton MJ, Buckingham JC, Flower RJ, Morris JF, Christian HC. Evidence for a role of the ATP-Binding cassette transporter A1 (ABCA1) in the externalization of annexin 1 from pituitary folliculostellate cells. *Endocrinology*. 2003; 144:1062–1073. [PubMed: 12586783]
19. Christian HC, Taylor AD, Morris JF, Goulding NJ, Flower RJ, Buckingham JC. Characterisation and localisation of lipocortin 1 binding sites in the anterior pituitary gland by fluorescence activated cell analysis/sorting. *Endocrinology*. 1997; 138:5341–5352. [PubMed: 9389519]
20. Ozawa H, Ito T, Ochiai I, Kawata M. Cellular localization and distribution of glucocorticoid receptor (GR) immunoreactivity and the expression of GR mRNA in the rat anterior pituitary gland: a combined double immunohistochemistry and *in situ* hybridization histochemical analysis. *Cell Tissue Res*. 1999; 295:207–214. [PubMed: 9931366]
21. Fauquier T, Guerineau NC, McKinney RA, Bauer K, Mollard P. Folliculostellate cell network: a route for long-distance communication in the anterior pituitary. *Proc Natl Acad Sci USA*. 2001; 98:8891–8896. [PubMed: 11438713]
22. Allaerts W, Vankelecom H. History and perspectives of pituitary folliculostellate cell research. *Eur J Endocrinol*. 2005; 153:1–12. [PubMed: 15994739]
23. Renner U, Gloddek J, Paez Pereda M, Arzt E, Stalla GK. Regulation and role of intrapituitary IL-6 production by folliculostellate cells. *Domestic Anim Endocrinol*. 1998; 15:353–362.
24. Tierney T, Patel R, Stead CAS, Leng L, Bucala R, Buckingham JC. Macrophage migration inhibitory factor is released from pituitary folliculostellate-like cells by endotoxin and dexamethasone and attenuates the steroid-induced inhibition of interleukin 6 release. *Endocrinology*. 2005; 146:35–43. [PubMed: 15388650]
25. Bilezikjian LM, Leal AMO, Blount AL, Corrigan AZ, Turnbull AV, Vale WW. Rat anterior pituitary FS cells are targets of IL-1beta and are a major source of intrapituitary follistatin. *Endocrinology*. 2003; 144:732–740. [PubMed: 12538636]
26. Hannon R, Croxtall JD, Getting SJ, Roviezzo F, Yona S, Paul-Clark MJ, Gavins FN, Perretti M, Morris JF, Buckingham JC, Flower RJ. Aberrant inflammation and resistance to glucocorticoids in annexin 1 *-/-* mouse. *FASEB J*. 2003; 17:253–255. [PubMed: 12475898]
27. Yona S, Buckingham JC, Perretti M, Flower RJ. Stimulus-specific defect in the phagocytic pathways of annexin 1 null macrophages. *Br J Pharmacol*. 2004; 142:890–898. [PubMed: 15197108]
28. Chatterjee BE, Yona S, Rosignoli G, Young RE, Nourshargh S, Flower RJ, Perretti M. Annexin 1-deficient neutrophils exhibit enhanced transmigration *in vivo* and increased responsiveness *in vitro*. *J Leukocyte Biol*. 2005; 78:639–646. [PubMed: 16000391]

29. Nakane, PK. Identification of anterior pituitary cells by immunoelectron microscopy. In: Tixier-Vidal, A.; Farquhar, M., editors. *The Anterior Pituitary Gland*. New York, NY: Academic Press; 1975. p. 134-158.
30. Christian HC, Morris JF. Rapid actions of estradiol on a subset of lactotrophs in male rat pituitary. *J Physiol*. 2002; 539:557–561. [PubMed: 11882687]
31. Cruz-Orive D, Weibel G. Recent stereological methods for cell biology: a brief survey. *Am J Physiol*. 1990; 258:L148–L156. [PubMed: 2185653]
32. Childs GV, Westlund KN, Tibolt RE, Lloyd JM. Hypothalamic regulatory peptides and their receptors: cytochemical studies of their role in regulation at the adenohypophyseal level. *J Electron Microscop Tech*. 1991; 19:21–41. [PubMed: 1660066]
33. Gertz BJ, Contreras LN, McComb DJ, Kovacs K, Tyrrell JB, Dallman MF. Chronic administration of corticotropin-releasing factor increases pituitary corticotroph number. *Endocrinology*. 1987; 120:381–388. [PubMed: 3023033]
34. McNicol AM, Kubba MA, McTeague E. The mitogenic effects of corticotrophin-releasing factor on the anterior pituitary gland of the rat. *J Endocrinol*. 1988; 118:237–241. [PubMed: 3262703]
35. Nolan LA, Thomas CK, Levy A. Enhanced anterior pituitary mitotic response to adrenalectomy after multiple glucocorticoid exposures. *Eur J Endocrinol*. 2003; 149:153–160. [PubMed: 12887293]
36. Loxley HD, Cowell AM, Flower RJ, Buckingham JC. Effects of lipocortin 1 and dexamethasone on the secretion of corticotrophin-releasing factors in the rat: in vitro and in vivo studies. *J Neuroendocrinol*. 1993; 5:51–61. [PubMed: 8485543]
37. Croxtall JD, Flower RJ. Lipocortin 1 mediates dexamethasone-induced growth arrest of the A549 lung adenocarcinoma cell line. *Proc Natl Acad Sci USA*. 1992; 89:3571–3575. [PubMed: 1533045]
38. Croxtall JD, Flower RJ. Antisense oligonucleotides to human lipocortin-1 inhibit glucocorticoid-induced inhibition of A549 cell growth and eicosanoid release. *Biochem Pharmacol*. 1994; 48:1729–1734. [PubMed: 7980642]
39. Perretti M, Solito E. Annexin 1 and neutrophil apoptosis. *Biochem Soc Trans*. 2004; 32:507–510. [PubMed: 15157173]
40. Kamal AM, Smith SF, De Silva Wijayasinghe M, Solito E, Corrigan CJ. An annexin 1 (ANXA1)-derived peptide inhibits prototype antigen-driven human T cell Th1 and Th2 responses in vitro. *Clin Exp Allergy*. 2001; 31:1116–1125. [PubMed: 11468004]
41. Kim SB, Yang WS, Lee OS, Lee KP, Park JS, Na DS. Lipocortin-1 inhibits proliferation of cultured human mesangial cells. *Nephron*. 1996; 74:39–44. [PubMed: 8883018]
42. Gold R, Pepinsky RB, Zettl UK, Toyka KV, Hartung HP. Annexin-1 suppresses activation of autoimmune T cell lines in the Lewis rat. *J Neuroimmunol*. 1996; 69:157–164. [PubMed: 8823388]
43. Croxtall JD, Waheed S, Choudhury Q, Anand R, Flower RJ. N-terminal peptide fragments of lipocortin-1 inhibit A549 cell growth and block EGF-induced stimulation of proliferation. *Int J Cancer*. 1993; 54:153–158. [PubMed: 8478141]
44. Gavins FN, Yona S, Kamal AM, Flower RJ, Perretti M. Leukocyte adhesive actions of annexin 1: ALXR- and FPR-related anti-inflammatory mechanisms. *Blood*. 2003; 101:4140–4147. [PubMed: 12560218]
45. John C, Flower RJ, Buckingham JC. Does annexin 1 act via the FPR receptor? *J Endocrinol*. 2001; 169:P150.
46. Childs GV, Rougeau D, Unabia G. Corticotropin-releasing hormone and epidermal growth factor: mitogens for anterior pituitary corticotropes. *Endocrinology*. 1995; 136:1595–1602. [PubMed: 7895669]
47. Sawada M, Suzumura A, Marunouchi T. Cytokine network in the central nervous system and its roles in growth and differentiation of glial and neuronal cells. *Int J Dev Neurosci*. 1995; 13:253–264. [PubMed: 7572279]
48. Akita S, Redhead C, Stefanescu L, Fine J, Tampanaru-Sarmesiu A, Kovacs K, Melmed S. Pituitary-directed leukaemia inhibitory factor transgene forms Rathke's cleft cysts and impairs

- adult pituitary function. A model for human Rathke's cysts. *J Clin Invest*. 1997; 99:2462–2469. [PubMed: 9153290]
49. Japon MA, Rubenstein M, Low MJ. In situ hybridization analysis of anterior pituitary hormone gene expression during fetal mouse development. *J Histochem Cytochem*. 1994; 42:1117–1125. [PubMed: 8027530]
50. Liu J, Lin C, Gleiberman A, Ohgi K, Herman T, Huang H-P, Tsai M-J, Rosenfeld MJ. Tbx19, a tissue selective regulator of POMC gene expression. *Proc Natl Acad Sci USA*. 2001; 98:8674–8679. [PubMed: 11447259]
51. Sasaki F, Wu P, Rougeau D, Unabia G, Childs GV. Cytochemical studies of responses of corticotropes and thyrotropes to cold and novel environment stress. *Endocrinology*. 1990; 127:285–297. [PubMed: 2163313]
52. Wells D, Wells K, Hannon R, Croxtall JD, Damazo AS, Oliani SM, Getting SJ, Parente L, Paul Clark MJ, Yona S, Gavins FNE, Martin J, Christian HC, Morris JF, Perretti M, Cover PO, John CD, Solito E, Buckingham JC, Flower RJ. The annexin 1 $-/-$ mouse: phenotypic studies. *Annexins*. 2004; 1:109–120.
53. Bethin KE, Vogt SK, Muglia LJ. Interleukin 6 is an essential corticotrophin-releasing hormone-independent stimulator of the adrenal axis during immune system activation. *Proc Natl Acad Sci USA*. 2000; 97:9317–9322. [PubMed: 10922080]
54. Spangelo BL, MacLeod RM, Isakson PC. Production of interleukin-6 by anterior pituitary cells in vitro. *Endocrinology*. 1990; 126:582–586. [PubMed: 2294005]

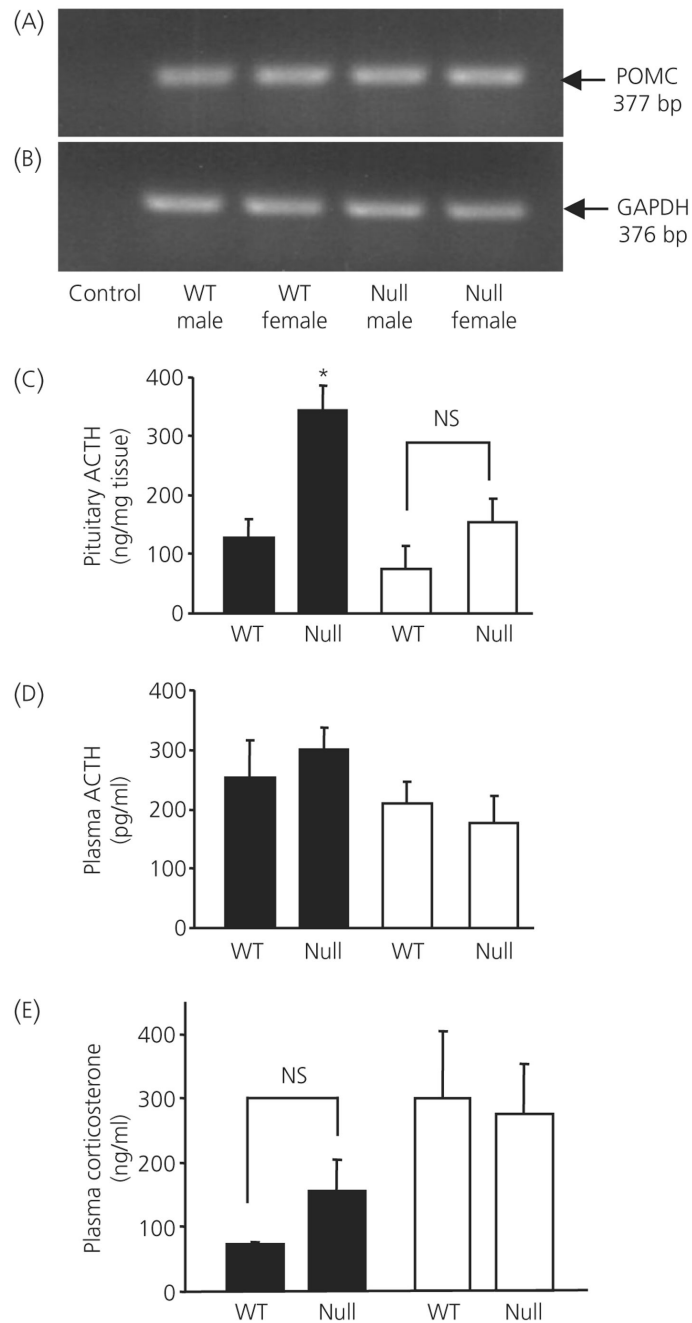


Fig. 1. Pituitary pro-opiomelanocortin (POMC) mRNA, adrenocorticotrophic hormone (ACTH) content, circulating ACTH and corticosterone in wild-type (WT) and ANXA1 null mice. Reverse transcriptase-polymerase chain reaction gels showing (A) POMC mRNA (predicted size 377 bp) and (B) GAPDH mRNA control (predicted size 376 bp) in wild-type and ANXA1 null anterior pituitary. Control lane is negative control. Histograms showing (C) pituitary ACTH content, (D) circulating ACTH and (E) circulating corticosterone in wild-type and ANXA1 null mice. Filled bars, male; open bars, female mice. Data are mean \pm SEM (n = 8 for all groups). *P < 0.05 versus wild-type of the same gender.

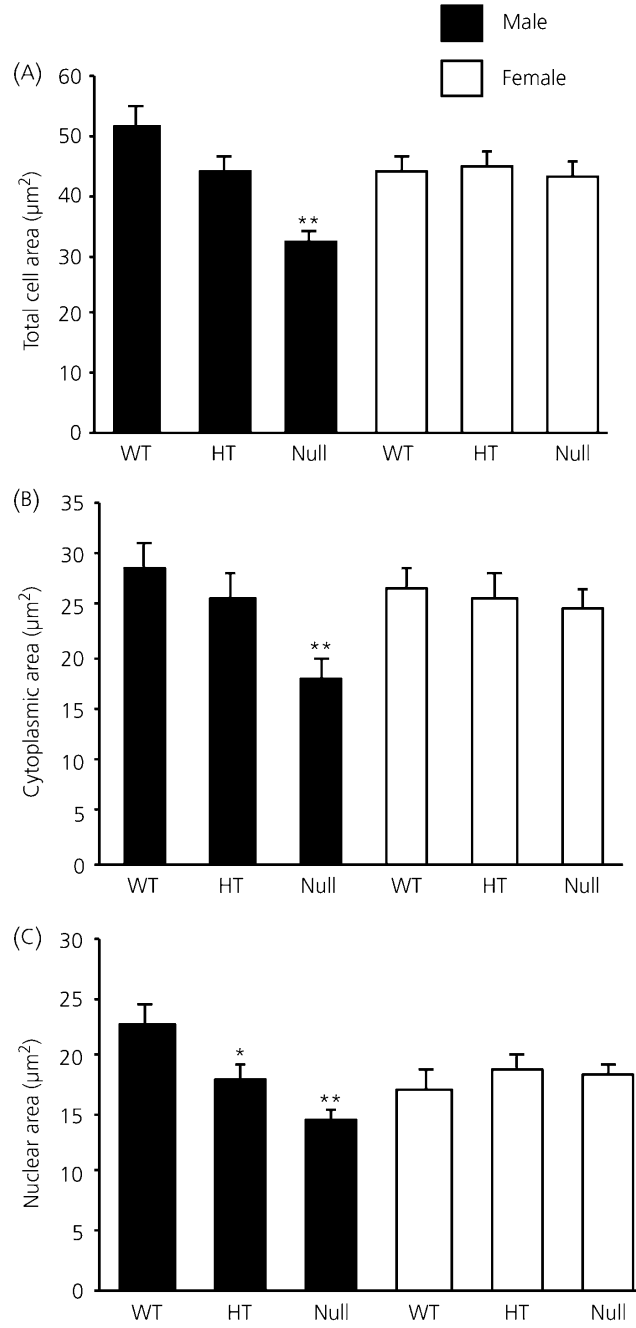


Fig. 2. Analysis of (A) cell size, (B) cytoplasmic area and (C) nuclear area in wild-type (WT), heterozygous (HT) and ANXA1 null anterior pituitary corticotrophs. Filled bars, male; open bars, female corticotrophs. Data are mean \pm SEM (n = 4 for all groups). *P < 0.05, **P < 0.01 versus wild-type of the same gender.

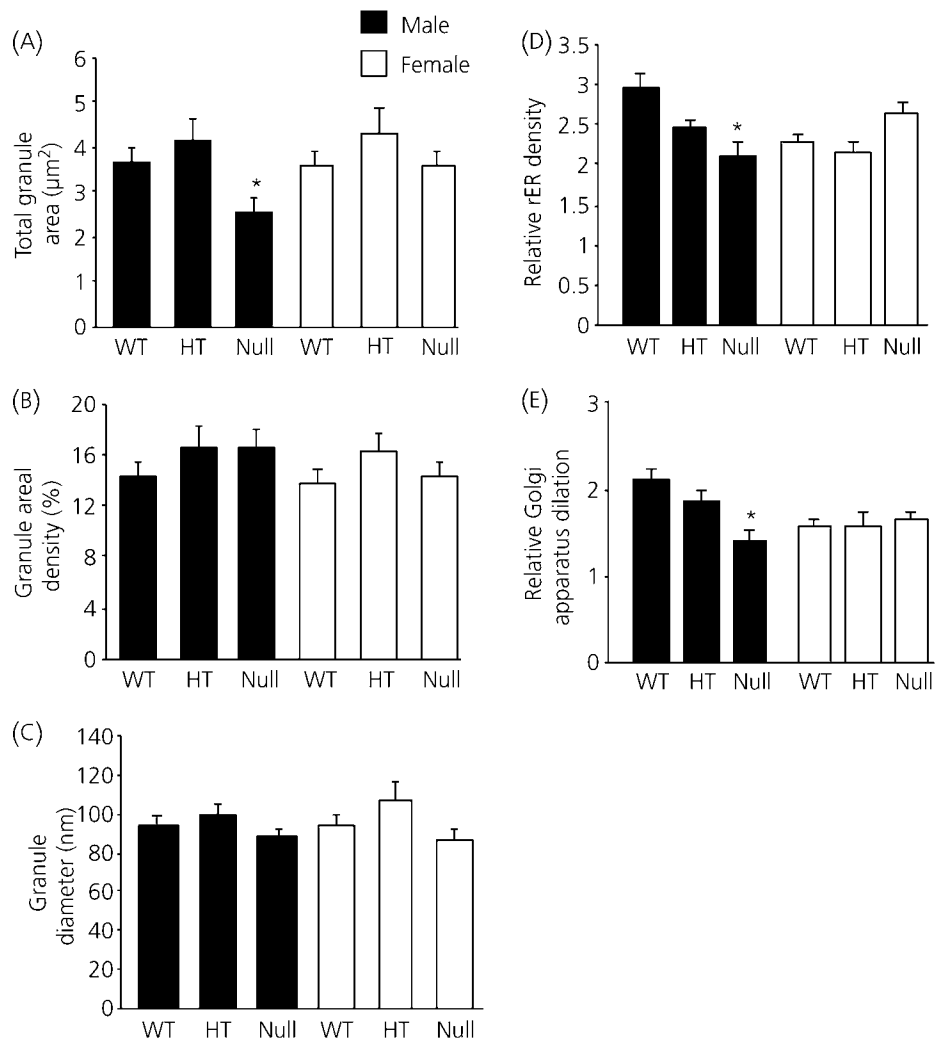


Fig. 3. Analysis of (A) total granule area, (B) granule areal density, (C) granule diameter, (D) rough endoplasmic reticulum (rER) areal density, and (E) Golgi apparatus dilation in corticotrophs from wild-type (WT), heterozygous (HT) and ANXA1-null mice. Filled bars, male; open bars, female corticotrophs. Data are mean \pm SEM (n = 4 for all groups). *P < 0.05 versus wild-type of the same gender.

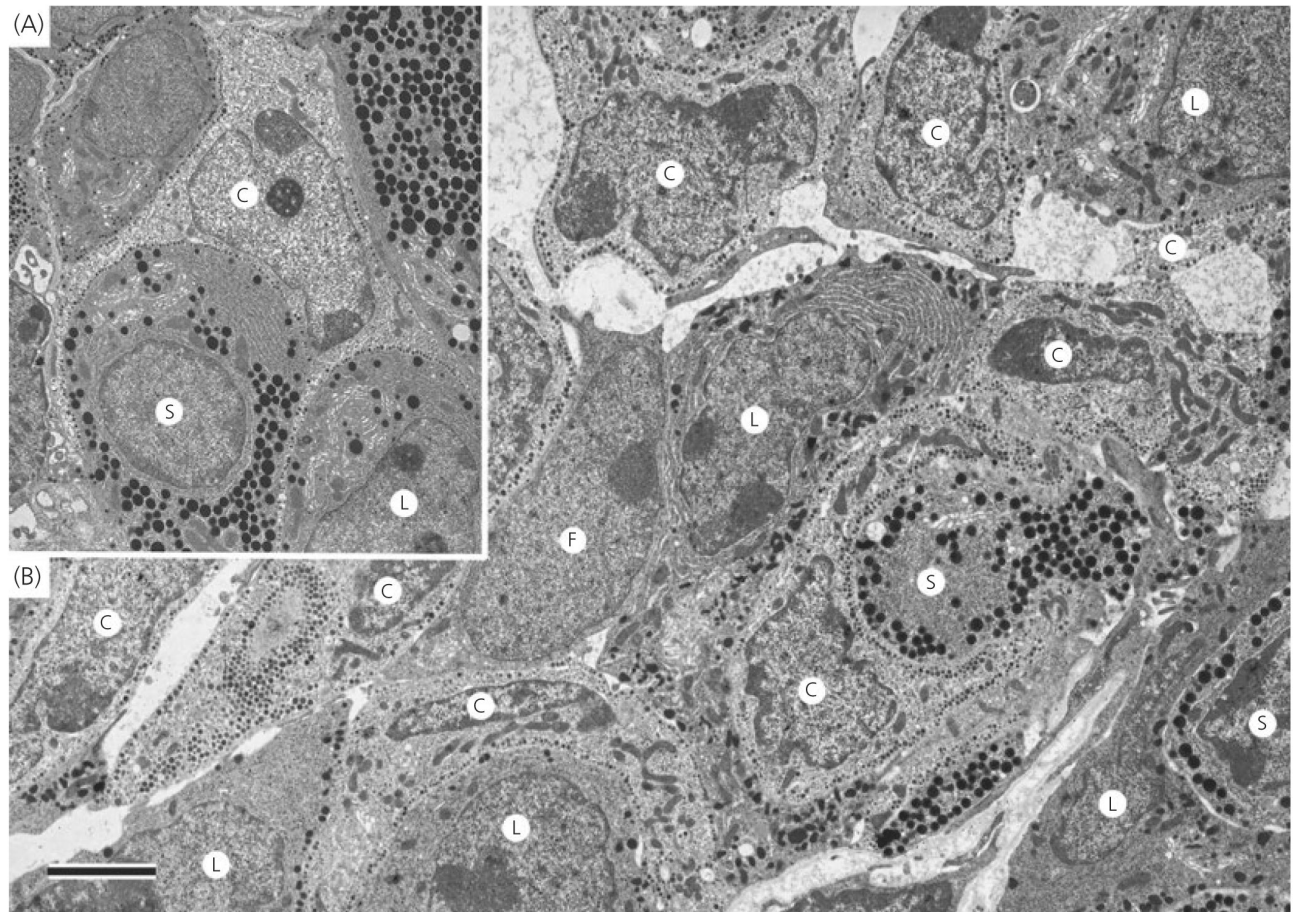


Fig. 4. Electron micrographs of anterior pituitary from male (A) wild-type and (B) ANXA1 null mice. In wild-type male mice, corticotrophs (c) were stellate, single and characterised by pale cytoplasm and peripheral secretory granules. In ANXA1 null male mice, many more immunoidentified corticotrophs were present, often in clusters. Their ultrastructural appearance was similar to that in wild-type mice. F, Folliculostellate cell; L, lactotroph; S, somatotroph. Scale bar = 2 μm .

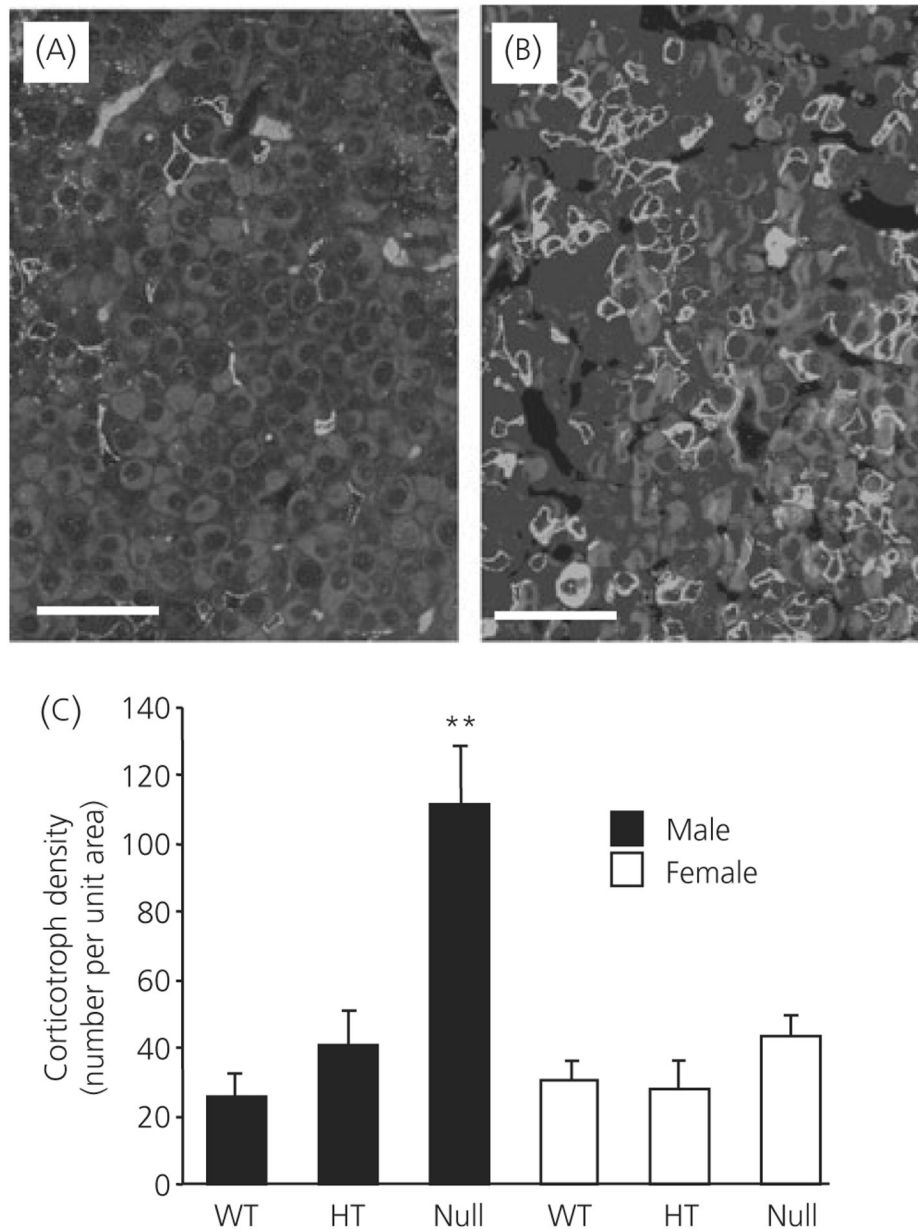


Fig. 5. Analysis of corticotroph cell density in wild-type (WT), heterozygote and ANXA1 null mice. Immunofluorescence detection of adrenocorticotrophic hormone-labelled corticotrophs in (A) wild-type and (B) ANXA1 null pituitary and (C) quantification of corticotroph cell density. Filled bars, male; open bars, female corticotrophs. Data are mean \pm SEM (n = 4 for all groups). **P < 0.05 versus wild-type of the same gender. Scale bars = 50 μ m.

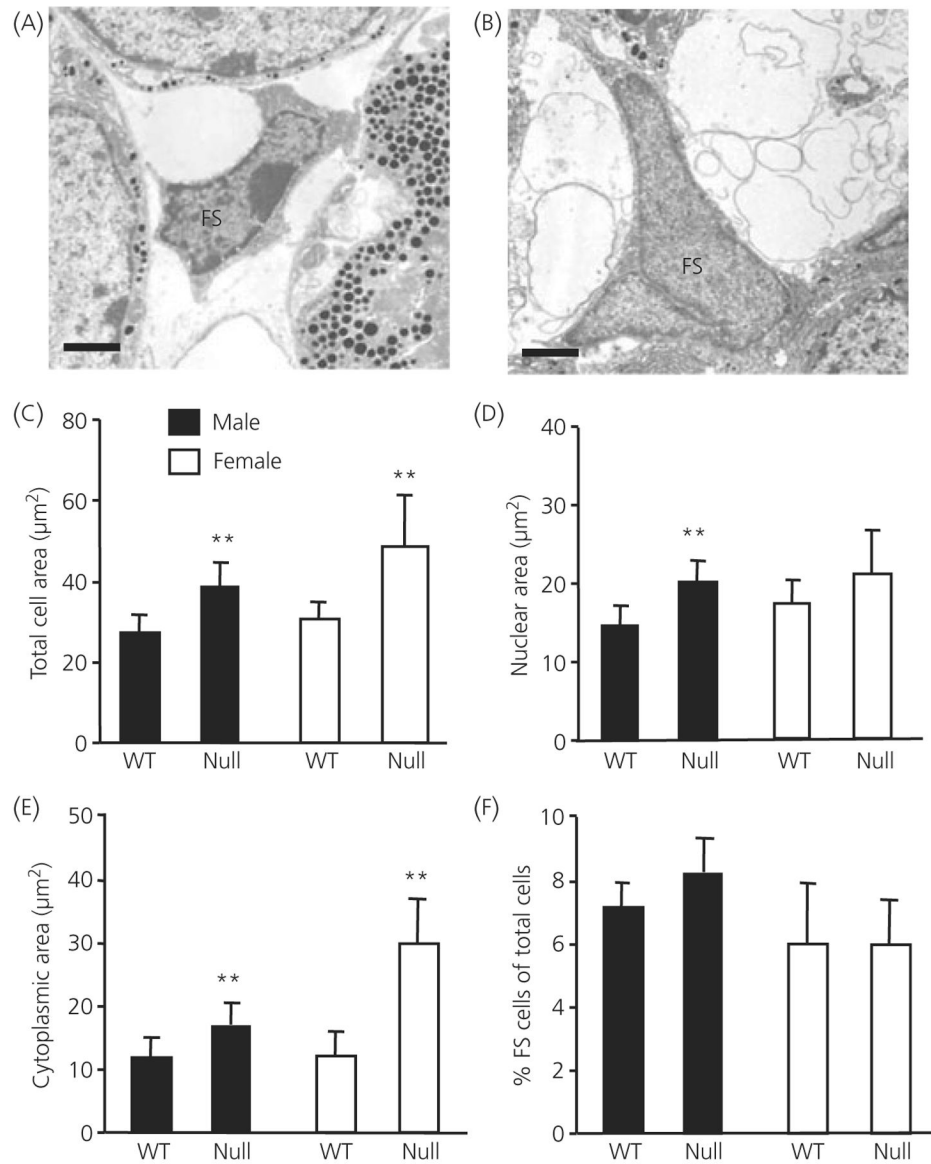


Fig. 6. Electron micrographs and analysis of folliculo-stellate (FS) cell size in wild-type (WT) and ANXA1 null mice. Micrographs illustrating (A) a typical male wild-type FS cell and (B) male ANXA1 null FS cell. Analysis of FS (C) cell area, (D) nuclear area, (E) cytoplasmic area and (F) FS cell density. Data are mean \pm SEM ($n = 4$ for all groups). ** $P < 0.05$ versus wild-type of the same gender. Scale bars = 1 μm .

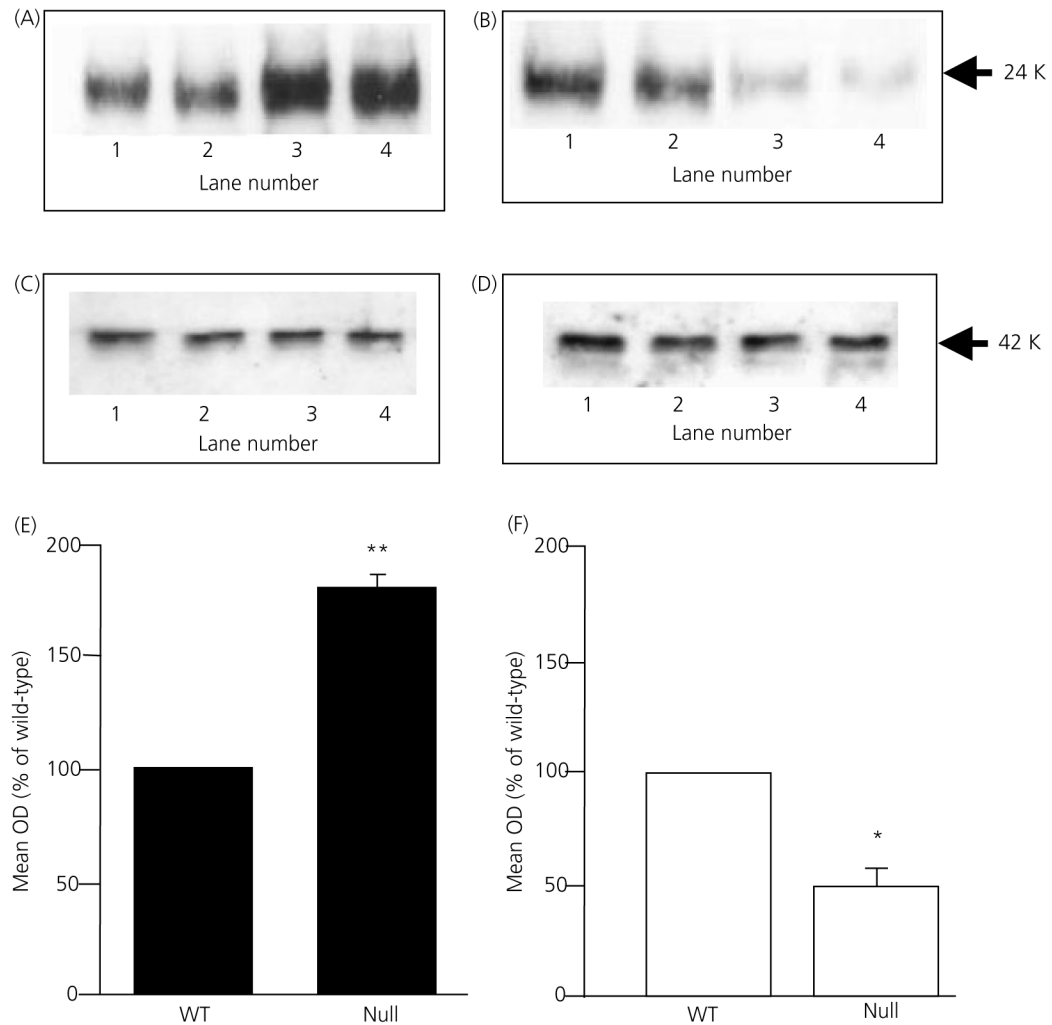


Fig. 7. Western blot analysis of interleukin (IL)-6 in anterior pituitary from ANXA1 wild-type (WT) and null mice. (A) IL-6 and (C) β -actin Western blots: wild-type male, lanes 1 and 2; ANXA1 null male, lanes 3 and 4; (B) IL-6 and (D) β -actin Western blots: wild-type female, lanes 1 and 2; ANXA1 null female, lanes 3 and 4. Total integrated densitometry data for male tissue (E) and female tissue (F). Data are mean \pm SEM ($n = 5$ experiments) and represent integrated densities for IL-6 expressed as percentage wild-type; * $P < 0.05$, ** $P < 0.01$ versus wild-type of the same gender.

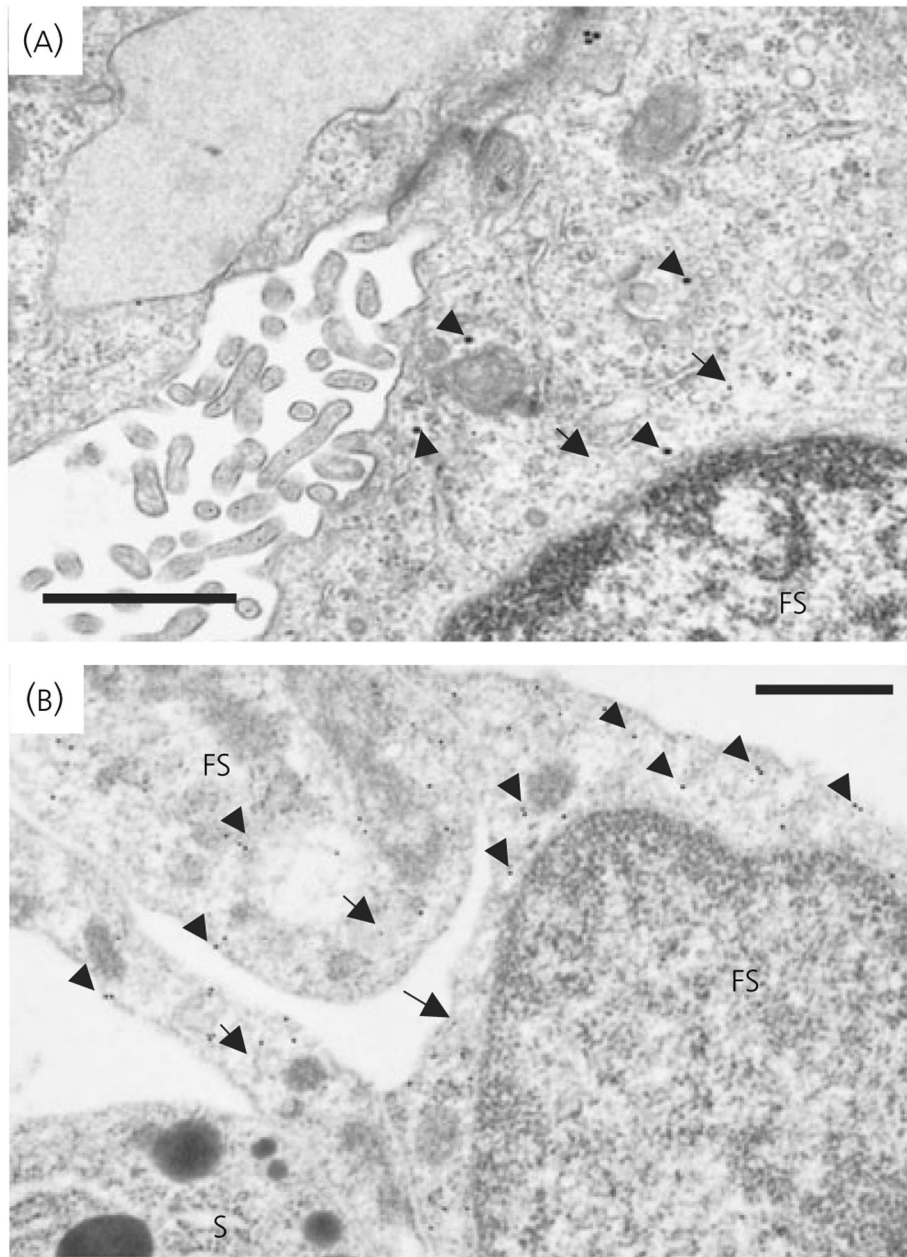


Fig. 8. Electron micrographs from freeze substituted (A) wild-type and (B) ANXA1 null male pituitary showing immunogold detection of interleukin (IL)-6 and S-100 in folliculo-stellate (FS) cells. IL-6 gold particles (15 nm; arrowheads) were scattered over the cytoplasm. Increased density of labelling was observed in ANXA1 null FS cells. S-100 gold particles (5 nm arrows) confirmed identification of FS cells. S, Somatotroph cell. Scale bars = 1 μ m.

Table 1
 Analysis of Type I and II Lactotrophs, Gonadotrophs and Somatotrophs in Male Wild-Type and ANXA1 Null Mice.

Animal	Cell area (μm^2)	Cytoplasmic area (μm^2)	Granule density (% cell area)	Granule diameter (nm)	Rough ER (units)	Density of cells (% total cells)
Type I lactotrophs						
Wild-type	41 \pm 3	23 \pm 2	26 \pm 2	270 \pm 20	1.03 \pm 0.1	7 \pm 1
ANXA1 null	43 \pm 4	23 \pm 2	34 \pm 3	285 \pm 22	1.7 \pm 0.1**	5 \pm 2
Type II lactotrophs						
Wild-type	41 \pm 4	20 \pm 2	30 \pm 2	81 \pm 3	0.87 \pm 0.1	8 \pm 2
ANXA1 null	43 \pm 4	24 \pm 2	29 \pm 2	89 \pm 2	1.43 \pm 0.1**	8 \pm 2
Gonadotrophs						
Wild-type	67 \pm 8	51 \pm 6	19 \pm 1	151 \pm 10	0.5 \pm 0.1	18 \pm 2
ANXA1 null	77 \pm 5	61 \pm 4	14 \pm 1	137 \pm 11	1.2 \pm 0.2**	19 \pm 2
Somatotrophs						
Wild-type	55 \pm 3	41 \pm 2	48 \pm 2	131 \pm 2	0.93 \pm 0.1	43 \pm 2
ANXA1 null	63 \pm 3	47 \pm 2	46 \pm 1	147 \pm 2	1.32 \pm 0.1**	45 \pm 3

Values represent mean \pm SEM (n = 4 animals).

** P < 0.01 versus wild-type of the same gender. ER, Endoplasmic reticulum.

Table 2

Quantification of Interleukin (IL)-6 Gold Particles in the FolliculoStellate Cells of Male and Female Wild-Type and ANXA1 Null Mice.

	IL-6 immunogold (gold particles/μm^2)
Wild-type, male	4.2 \pm 0.4
ANXA1 null, male	8.7 \pm 1.1 **
Wild-type, female	4.6 \pm 0.5
ANXA1 null, female	2.3 \pm 0.3 *

The data are expressed as gold particles per μm^2 within the total cytoplasmic area. Values represent mean \pm SEM (n = 4 animals).

* P < 0.05,

** P < 0.01 versus wild-type of the same gender.